ISBN: 978-3-95450-197-7 doi:10.18429/JACoW-RUPAC2018-THPSC47

CHARACTERISTICS OF LASER-PLASMA ION SOURCE BASED ON A CO_2-LASER FOR HEAVY ION ACCELERATORS AT ITEP

A.A. Losev, A. Balabaev, I. Hrisanov, T. Kulevoy, Yu. Satov, A. Shumshurov, A. Vasilyev
NRC «Kurchatov Institute» - ITEP, 117259 Russia, Moscow

Abstract

The design of laser-plasma heavy ion source is described. This ions source is supposed to operate at I-3 and I-4 accelerators at ITEP. Characteristics of ion component of plasma produced by pulses of the CO_2 laser were studied, when irradiating a solid carbon target at power density of $10^{11} \div 10^{12}$ W/cm^2. Time-of-flight technique using a high-resolution electrostatic energy analyzer was applied to explore charge state and energy distribution as well as partial currents of carbon and tungsten ions. Some results of investigation of influence of cavern formation on charge state of generated ions are presented. This work is of considerable interest in a wide area of applications of accelerated particle beams, including fundamental studies of state of matter in particle colliders (NICA project at JINR), radiation damage simulation and hadron therapy for cancer treatment. The goal of this work is to investigate characteristics of ions in expanding laser plasma and find optimal conditions of target illumination and ion beam extraction. This research is valuable for adapting an intensive beam from laser ion source to the accelerator, improving acceleration efficiency and rising the amount of accelerated particles.

SCHEMATIC DIAGRAM OF THE HIGH CURRENT ION INJECTOR

Schematic diagram of the high current heavy ion I-4 (ITEP) is shown on Fig. 1.

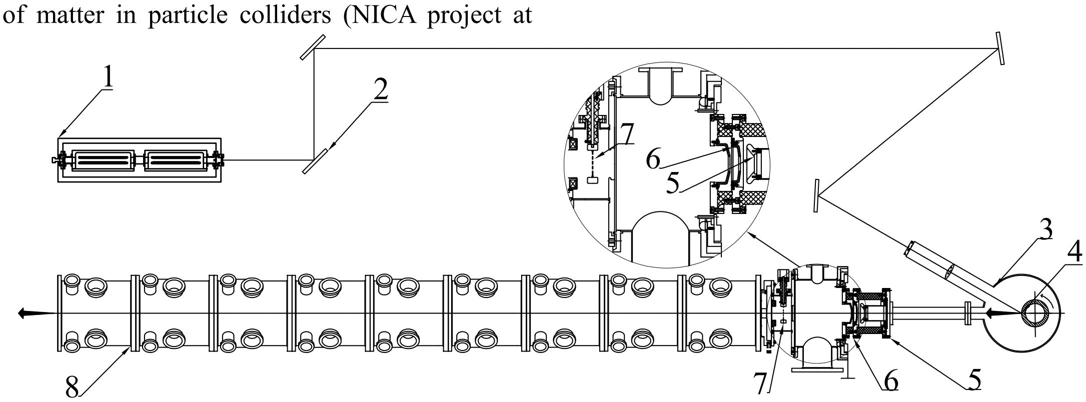

Figure 1: Schematic diagram of ion injector I-4.

It consists of two-modules CO_2 pulsed laser generator *1* which radiation is transported by copper mirrors *2* to the entrance tube of the vacuum chamber *3* that has the internal diameter of 350 mm. Then the laser beam is focused to the target *4* with the spherical lens. The target rotates around the geometrical axis and shifts up and down during operation to avoid a crater formation in the target material. The laser beam falls on the target angularly (30º) but the surface normal coincides with the time of flight tube axis and laser plasma expansion direction. The extraction system consists of three electrodes: positive *5*, negative *6* and grounded (interelectrode distances are 40 and 20 mm, accordingly). Positive extraction electrode is placed at the distance 1680 mm from the target. Its passage opening of 40 mm is closed by the grid. Gridded lens *7* is used to match the ion beam with the RFQ section *8* entrance. The RFQ section main characteristics are frequency–81.36 MHz, z/A≥1/3, injection energy–0.02 MeV/u, output energy–1.6 MeV/u, maximum ion current–100 mA. The system operates in repetition rate mode up to 0.2 Hz.

CHARACTERISTICS OF LASER BEAM

CO_2 laser setup [1] operates at a high level of the specific energy deposition into a self-sustained discharge. It provides laser beam with high quality of spatial and temporal characteristics:

- pulse energy – 7 J
- peak power – up to105 MW
- FWHM duration – 30 ns
- Beam divergence – close to diffraction limit

These parameters are reproduced during long term operation.

Flat mirrors transport the laser beam into the vacuum chamber. Then laser radiation is focused on the target surface by exchangeable spherical lenses with different focal length to vary power density in the range of $8{\cdot}10^{10} \div 8{\cdot}10^{11}$ W/cm^2. A typical shape of the spatial distribution of the energy density in the focal spot is close to Gaussian and its width is between 200 ÷ 600 µm.

ISBN: 978-3-95450-197-7 doi:10.18429/JACoW-RUPAC2018-THPSC47

TIME OF FLIGHT PLASMA DIAGNOSTICS

The time-of-flight technique is applied to study ion component of the laser plasma plume. Use of an electrostatic energy analyzer allows reconstructing charge state and energy distributions of ions, and their partial currents. Energy resolution $\Delta E/E$ of the instrument achieved is estimated as $\Delta E/E \approx 8{\cdot}10^{-4}$ [2]. The 143EM secondary electron multiplier with one-electron response time of 3 ns was used as the particle detector

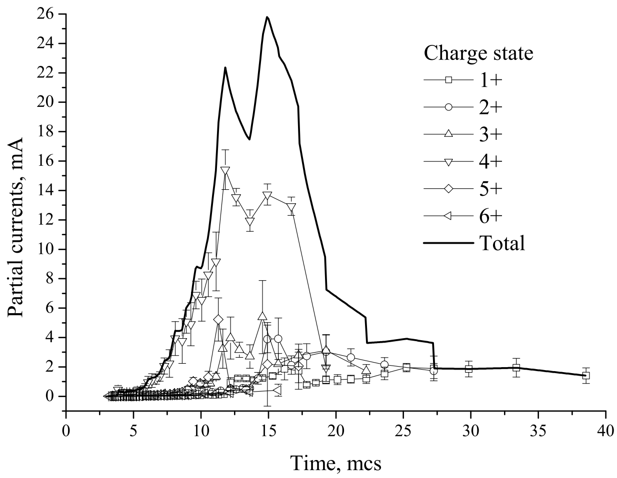

Figure 2: Partial currents of carbon ions. Target was shifted after each laser pulse.

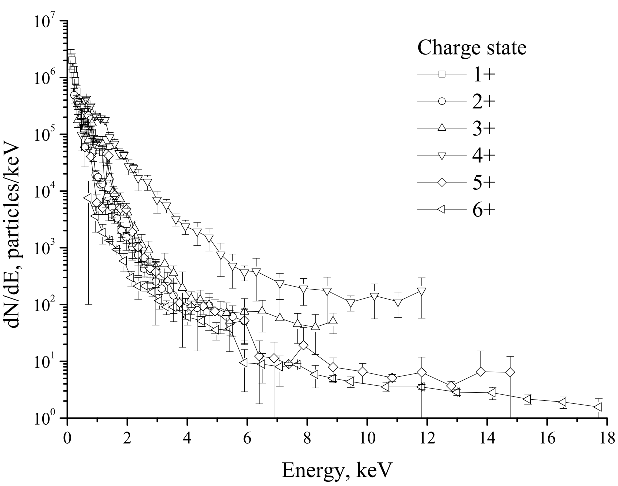

Figure 3: Energy distribution of carbon ions. Target was shifted after each laser pulse.

Energy distributions and partial currents of carbon ions emitted from laser produced plasma plume are presented on Figs. 2 and 3. These results were obtained when target was shifted by 500 µm after each laser pulse. The results presented on Figs. 4 and 5 were obtained with fixed target after 600 laser pulses.

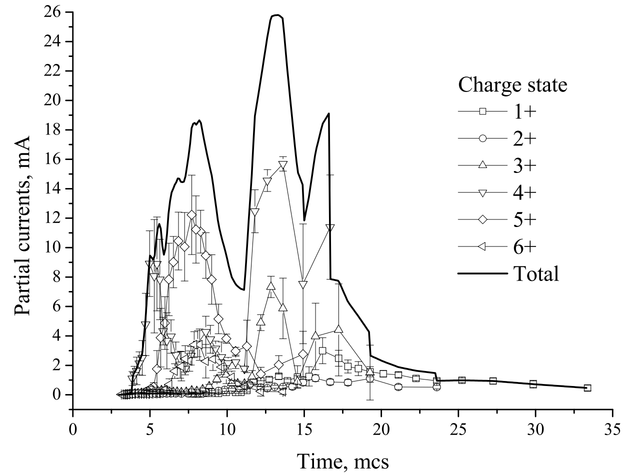

Figure 4: Partial currents of carbon ions. Target was fixed.

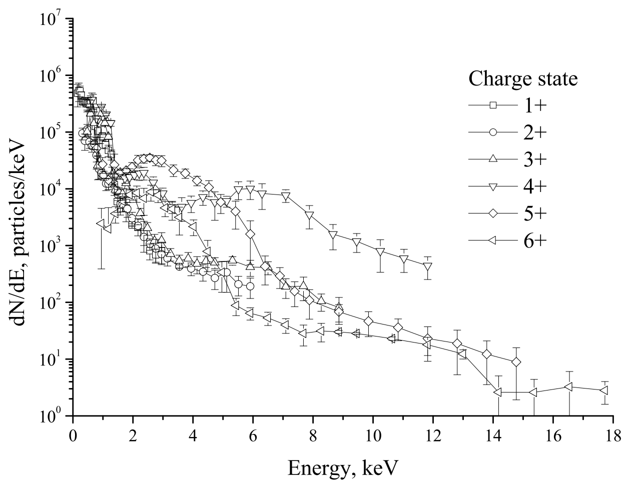

Figure 5: Energy distribution of carbon ions. Target was fixed.

Figure 6 shows the dependence of $C^{3+} \div C^{5+}$ ion signal amplitude on time of operation with fixed target. Ion energy is set to E = 600·Z eV. A 1.5 mm deep cavern was created on the surface of the target.

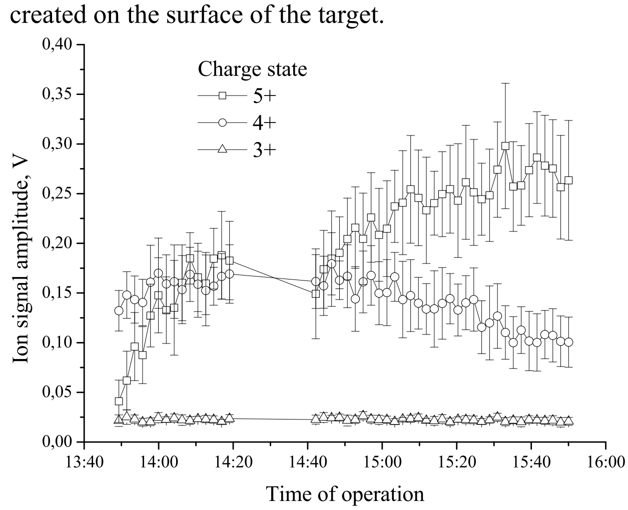

Figure 6: Dependence of ion signal amplitude on time of operation with fixed target.

ISBN: 978-3-95450-197-7 doi:10.18429/JACoW-RUPAC2018-THPSC47

Figure 7 shows the difference in charge state distribution for conditions with fixed and moving target. This effect can be explained by difference in distributions of plasma density and temperature along plasma expansion axis.

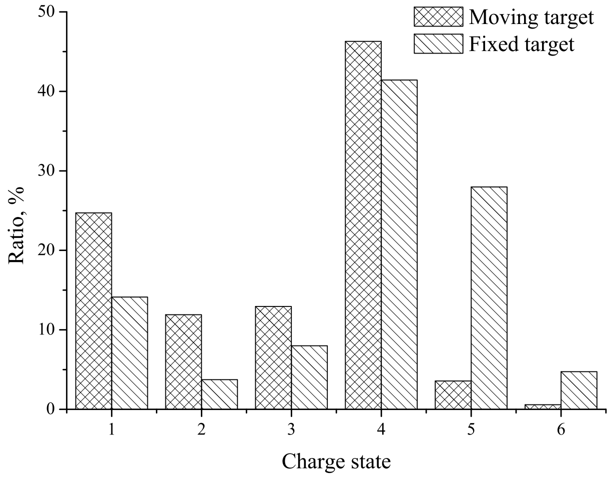

Figure 7: Charge state distributions measured with fixed and moving target.

Another target material for ion source was tungsten. Ions with charge state up to +20 were detected. Charge state distribution of tungsten ions is presented on Fig. 8.

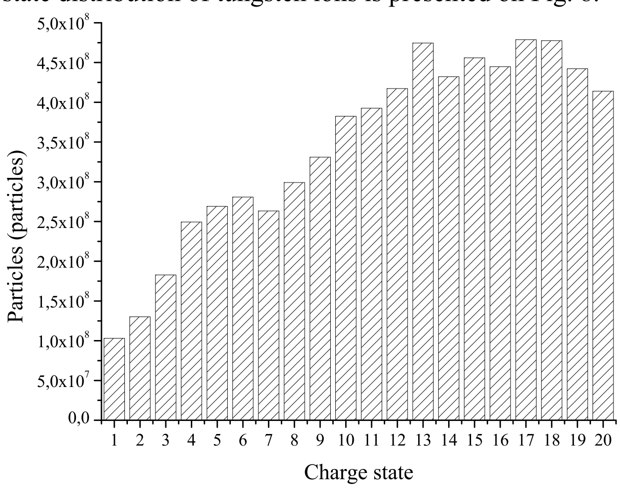

Figure 8: Charge state distribution in tungsten ion plasma.

Number of particles corresponds to 1 mA of extracted current, secondary emission coefficient is neglected.

BEAM EXTRACTION AND ACCELERATION

Beam extraction system consists of three electrodes. The positive electrode has a grid (transparency: 90 %, cell dimensions: 0.5 mm × 0.5 mm) and an exchangeable 10 mm diaphragm installed. To match C^{4+} ion beam energy into the RFQ the positive electrode has to be at +60 kV potential relative to ground. Extraction voltage is increased by the negative electrode. Ion beam current was measured by a Faraday cup placed behind the ground electrode of the extraction. +1.5 kV potential was applied to the cup to suppress secondary electron emission. Results of this measurement were used to calculate number of particles in single ion beam pulse: $7.3 \cdot 10^{11}$ particles in total, 46 % of them are C^{4+}. The “pepper-pot” technique with CCD-camera was used to measure beam emittance [3].

Temporal shape of total carbon ion beam current is presented on Fig. 9. Peak value is 25.8 mA.

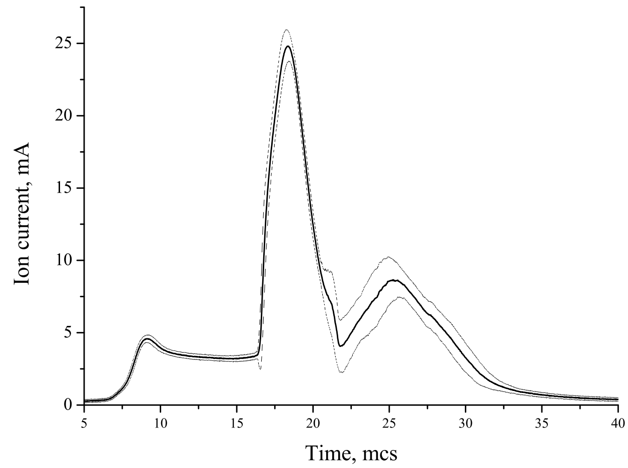

Figure 9: Total ion current at input of the RFQ.

Measured emittance values are about 520π mm·mrad along y-axis and 560π mm·mrad along x-axis for total ion beam current. Figure 10 represents total ion beam current at the output of the RFQ. Its peak value is 7.8 mA

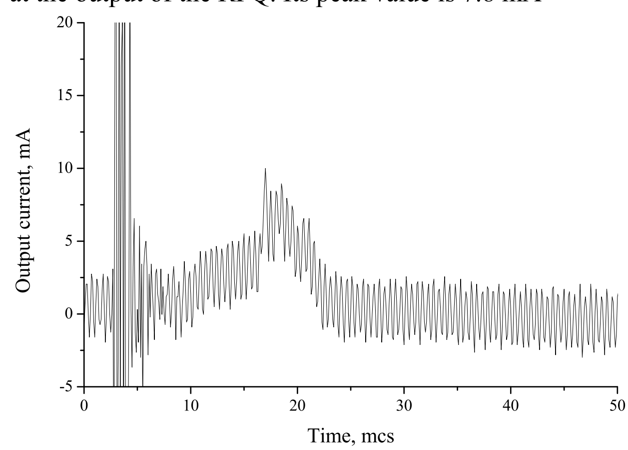

Figure 10: Total ion current at output of the RFQ.

REFERENCES

[1] Yu. A. Satov et al, Instrum. Exp. Tech. 59, 2016, pp. 412-419
[2] Yu. A. Satov et al,Instrum. Exp. Tech. 60, 2017, pp.556-561
[3] D. Liakin et al, Rev. Sci. Instr. 81, 2010, p. 02B719